1    The transcription factor Zt107320 affects the dimorphic switch, growth and virulence of the fungal

2    wheat pathogen *Zymoseptoria tritici*

3

4    Michael Habig, Sharon Marie Bahena-Garrido[#], Friederike Barkmann, Janine Haueisen and Eva
5    Holtgrewe Stukenbrock[*]

6

7    Environmental Genomics, Christian-Albrechts University of Kiel and Max Planck Institute for

8    Evolutionary Biology, Plön, Germany,

9

10    # Current address:

11    #National Research Institute of Brewing, 3-7-1 Kagamiyama, Higashi-Hiroshima, 739-0046 Japan

12

13

14    *corresponding author: estukenbrock@bot.uni-kiel.de

15

16    Running head: Zt107320 regulates virulence in *Z. tritici*

17

18    Keywords: Fungal dimorphism, incompatible host, Septoria leaf blotch, gene expression, pycnidia

19    formation

20

21    Word count: 6136

22

## Summary

*Zymoseptoria tritici* is a filamentous fungus causing Septoria tritici blotch in wheat. The pathogen has a narrow host range and infections of grasses other than susceptible wheat are blocked early after stomatal penetration. During these abortive infections the fungus shows a markedly different expression pattern. However, the underlying mechanisms causing differential gene expression during host and non-host interaction are largely unknown, but likely include transcriptional regulators responsible for the onset of an infection program in compatible hosts. In the rice blast pathogen *Magnaporthe oryzae*, MoCOD1, a member of the fungal Zn(II)$_2$Cys$_6$ transcription factor family, has been shown to directly affect pathogenicity. Here, we analyse the role of the putative transcription factor Zt107320, a homolog of MoCOD1, during infection of compatible and incompatible hosts by *Z. tritici*. We show for the first time that *Zt107320* is differentially expressed in host versus non-host infections and that lower expression corresponds to an incompatible infection of non-hosts. Applying reverse genetics approaches we further show that Zt107320 regulates the dimorphic switch as well as the growth rate of *Z. tritici* and affects fungal cell wall composition *in vitro*. Moreover, Δ*Zt107320* mutants showed reduced virulence during compatible infections of wheat. We conclude that Zt107320 directly influences pathogen fitness and propose that Zt107320 regulates growth processes and pathogenicity during infection. Our results suggest that this putative transcription factor is involved in discriminating compatible and non-compatible infections.

## Introduction

The fungus *Zymoseptoria tritici* (synonym *Mycosphaerella graminicola*) infects wheat and causes the disease Septoria tritici blotch. The pathogen is found worldwide where wheat is grown and can cause severe reduction in yield (Fones and Gurr, 2015). Upon infection, the fungus enters the leaf through stomata and establishes a hyphal network in the mesophyll. It propagates without causing visual symptoms for 7-14 days before inducing necrosis and producing pycnidia – asexual fructifications, where pycnidiospores are produced that can spread via contact or rain-splash to neighbouring leaves (Brading *et al.* 2002; Kema, G. H. J. *et al.* 1996; Ponomarenko A. S.B. Goodwin, G.H.J. Kema, 2011). *Z. tritici* has a heterothallic mating system and meiosis leads to the production of wind-borne ascospores that are considered to be the main primary inoculum (Kema *et al.* 1996; Morais *et al.* 2016; Ponomarenko A. S.B. Goodwin, G.H.J. Kema, 2011). Recently, we could show that chromosomal inheritance is characterised by frequent chromosome losses and rearrangements during mitosis and a drive of accessory chromosomes during meiosis (Habig *et al.* 2018; Möller *et al.* 2018), which may contribute to the genomic variation observed for *Z. tritici* (Grandaubert *et al.* 2017; Hartmann *et al.* 2017). Under experimental conditions, the fungus has a narrow host range infecting wheat and shows abortive infections on closely related non-host grass species like *Triticum monococcum* (Jing *et al.* 2008) and *Brachypodium distachyon* (Kellner *et al.* 2014; O'Driscoll *et al.* 2015). However, the underlying determinants of host specialisation and host specificity of *Z. tritici* are largely unknown.

A previous study comparing the expression profiles of *Z. tritici* between early infection (4 days post infection) of the compatible host *T. aestivum* and the non-host *B. distachyon* revealed a set of 289 genes that were similarly expressed in the two hosts, but differentially expressed compared to growth in axenic culture (Kellner *et al.* 2014). These genes are likely crucial for *Z. tritici* during stomatal penetration that occurs in same way in both hosts. However, 40 genes showed differential expression between host and non-host infections (Kellner *et al.* 2014) and are possibly involved in the discrimination of compatible and non-compatible host-pathogen interactions. The signalling and

3

68    regulatory networks responsible for these differential expression patterns are however unknown.

69    One of the differentially expressed genes encodes the putative transcription factor Zt107320.

70    Expression of *Zt107320* was significantly increased during infection of *T. aestivum* compared to the

71    early infection of *B. distachyon* (Kellner *et al.* 2014) suggesting a host-dependent regulation of the

72    gene.

73    *Zt107320* encodes a putative transcription factor belonging to the $Zn(II)_2Cys_6$ family. This gene family

74    of transcription factors is exclusive to fungi (MacPherson *et al.* 2006; Pan and Coleman, 1990) and

75    many members play an important role in the regulation of fungal physiology. For example, $Zn(II)_2Cys_6$

76    transcription factors in *Magnaporthe oryzae*, *Fusarium oxysporum*, *Leptosphaeria maculans,*

77    *Parastagonospora nodorum* and *Pyrenophora tritici-repentis* are involved in the regulation of fungal

78    growth and pathogenicity (Fox *et al.* 2008; Galhano *et al.* 2017; Imazaki *et al.* 2007; Lu *et al.* 2014;

79    Rybak *et al.* 2017). Interestingly, the homolog of *Zt107320* in the rice blast pathogen *M. oryzae*,

80    MoCOD1, was shown to affect conidiation and pathogenicity (Chung *et al.* 2013). *MoCOD1* was found

81    to be upregulated during conidiation and appressorium formation at 72h post infection.

82    Furthermore, the deletion mutant Δ*MoCOD1* showed defects in conidial germination and

83    appressorium formation. *In planta*, the mutant Δ*MoCOD1* was attenuated in extending growth from

84    the first-invaded cells and caused markedly reduced symptoms when compared to the wildtype

85    (Chung *et al.* 2013).

86    Transcription factors, in general, regulate expression by integrating various signalling pathways and

87    represent interesting targets for dissecting causes and mechanisms of pathogenicity and host

88    specificity. In *M. oryzae,* a systemic approach was applied to characterise all 104 members of the

89    $Zn(II)_2Cys_6$ family of transcription factors. Of these, 61 were shown to be involved in fungal

90    development and pathogenicity (Lu *et al.* 2014). Similarly, in the head blight causing fungus *Fusarium*

91    *graminearum* 26% of 657 tested transcription factors had an effect on the tested phenotypes

92    mycelial growth, conidia production and toxin production (Son *et al.* 2011). In summary, a number of

93    transcription factors, which play important roles in host infection and pathogenesis, have been

4

94    identified for several important crop pathogens (Chen *et al.* 2017; Okmen *et al.* 2014; Xiong *et al.*

95    2015; Zhang *et al.* 2018; Zhuang *et al.* 2016). In *Z. tritici* however, only few regulatory genes have

96    been characterised. Recently, two transcription factors ZtWor1 (Mirzadi Gohari *et al.* 2014) and ZtVf1

97    (Mohammadi *et al.* 2017) were shown to be important regulators of development and virulence of *Z.*

98    *tritici* during compatible infections of wheat, highlighting how transcription factors can be used to

99    identify and dissect aspects of pathogenicity. ZtWor1 has been functionally characterised and

100   appears to be involved in the cAMP-dependent pathway, upregulated during the initiation of

101   colonization and involved in regulating effector genes (Mirzadi Gohari *et al.* 2014). ZtVf1, a

102   transcription factor belonging to the $C_2$-$H_2$ subfamily is required for virulence and its deletion leads to

103   lower pycnidia density within lesions. Decreased virulence appears to be due to a reduced

104   penetration frequency and impaired pycnidia differentiation (Mohammadi *et al.* 2017)

105   Based on the close homology of *Zt107320* to *MoCOD1* and its significantly different expression

106   profile during host and non-host infections, we hypothesized that Zt107320 plays an important role

107   during early wheat infection of *Z. tritici*. Our results confirm that Zt107320 affects virulence of *Z.*

108   *tritici* during compatible infections and regulates the dimorphic switch as well as growth rate and cell

109   wall properties of this important fungal plant pathogen.

110

5

## Results

### Phylogenetic analysis of Zt107320

In order to determine the distribution of homologs of Zt107320 we performed a similarity search on

the protein level among putative fungal transcription factors. Among the 30 best matches 17 are

found among either plant pathogens or plant associated fungal organisms, however this association

does not appear to be monophyletic (fig 1 a). Among the thirty best hits, the *M. oryzae* homolog

MoCod1 and the *Alternaria brassicola* homolog AbPf2 have been functionally analysed. Deletion of

the *AbPf2* resulted in non-pathogenic strains (Cho *et al.* 2013). In the wild-type expression of *AbPf2*

decreased after initial colonization of host tissues and the authors conclude that AbPf1 regulates

pathogenesis (Cho *et al.* 2013). Among these highly conserved putative transcription factors two

protein domains are shared: Zn(2)-C6 fungal-type DNA binding domain superfamily (IRP036864) and

the transcription factor domain (IRP007219), indicating a functional role of the putative transcription

factors (see fig. 1 b). Zt1073120 is therefore homologous to several predicted transcription factors in

other fungal species, including some that have been associated with pathogenicity in plant

pathogenic species, indicating a similar regulatory role of this protein in *Z. tritici*.
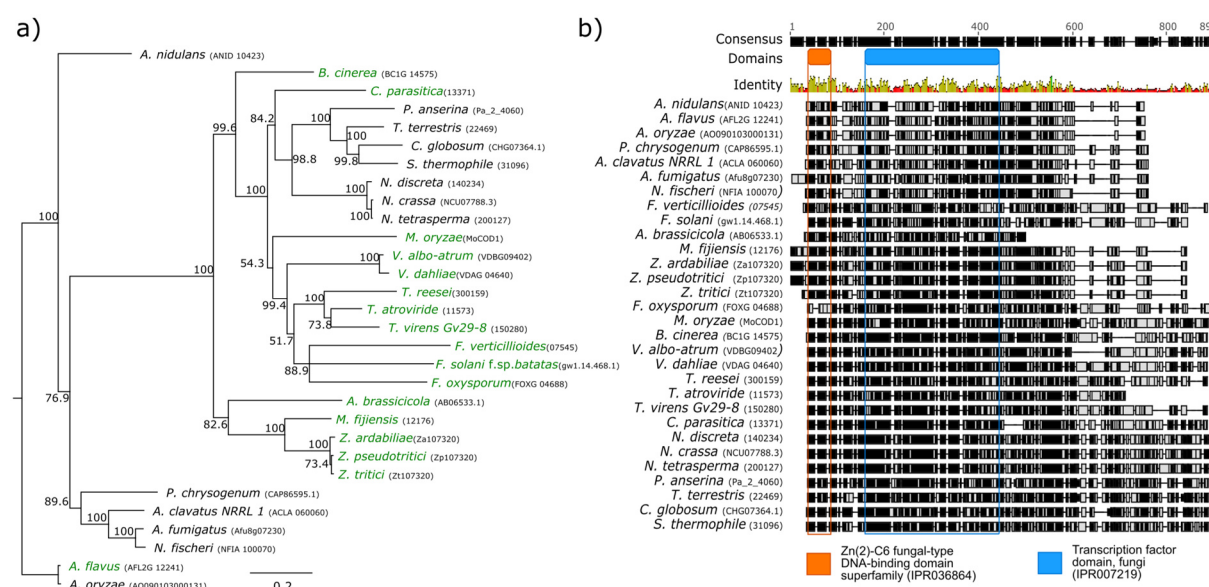


**Figure 1. Homology of Zt107320 among fungal transcription factors.** a) Phylogenetic tree based on
30 sequences showing the highest similarity with Zt107320 on the protein level, including the
orthologs in the sister species *Z. pseudotritici* and *Z. ardabiliae*. The phylogenetic tree was

6

131 constructed using MUSCLE alignments (Edgar, 2004) with Neighbour-Joining upon a consensus tree
132 with 1000 bootstrapping iterations. Support of nodes by percentage of bootstrapping iterations is
133 indicated. Species considered to be associated with plants are indicated in green. B) MUSCLE
134 alignment of homologous sequences to Zt107320 indicating regions according to their identity with
135 the consensus sequence. The localisations of two functional domains, identified using InterProScan,
136 in the consensus sequence are indicated.

137

138

139 **Infections of *Z. tritici* are blocked in the substomatal cavities during incompatible interaction with**

140 ***B. distachyon* coinciding with reduced expression of *Zt107320***

141 To study compatible and incompatible infections of *Z. tritici* in more detail, we inoculated leaves of

142 12-14 days old seedlings of *T. aestivum* (cultivar Obelisk) and *B. distachyon* (ecotype Bd21), and

143 analysed the infection development by confocal microscopy. Fungal cells germinated upon contact

144 with the leaf surface and developed infection hyphae. In contrast to previous observations (O'Driscoll

145 *et al.* 2015), we found that *Z. tritici* infection hyphae entered into open *B. distachyon* stomata at four

146 days post inoculation (dpi). However, further infection development of *Z. tritici* was blocked in the

147 substomatal cavities of *B. distachyon* leaves (fig 2a), similar to phenotypes previously observed in

148 incompatible interactions with einkorn wheat (Jing *et al.* 2008). Consequently, *Z. tritici* hyphae did

149 not colonize the mesophyll tissue of *B. distachyon*, no necrotic lesions developed, and no asexual

150 pycnidia formed. Interestingly, fungal growth was completely halted and no further growth was

151 observed, even when leaves were examined five weeks post inoculation (fig 2a). In contrast,

152 compatible infection of *Z. tritici* on the wheat cultivar Obelisk was characterised by previously

153 described infection stages (Haueisen *et al.* 2019). Penetration of leaf stomata at 4 dpi was followed

154 by the establishment of a hyphal network in the mesophyll tissue until 7-11 dpi and subsequently the

155 switch to necrotrophy when biomass increased substantially resulting in the formation of pycnidia

156 (fig 2a).

157

7

158     Previously, comparative transcriptome analyses during *Z. tritici* infection of the host *T. aestivum* and

159     the non-host *B. distachyon* identified 40 differentially expressed genes at 4 dpi (Kellner *et al.* 2014).

160     Building on this expression analysis, we focused on the putative transcription factor Zt107320 and

161     validated the expression kinetics of *Zt107320* by RT-qPCR. We confirmed differential expression at 8

162     dpi (fig 2b). Expression in the non-host *B. distachyon* was greatly reduced at 8 dpi compared to

163     expression in axenic cultures, whereas the expression of *Zt107320* during a compatible infection of

164     the host *T. aestivum* was strongly upregulated during the course of the infection until 21 dpi.

165

166
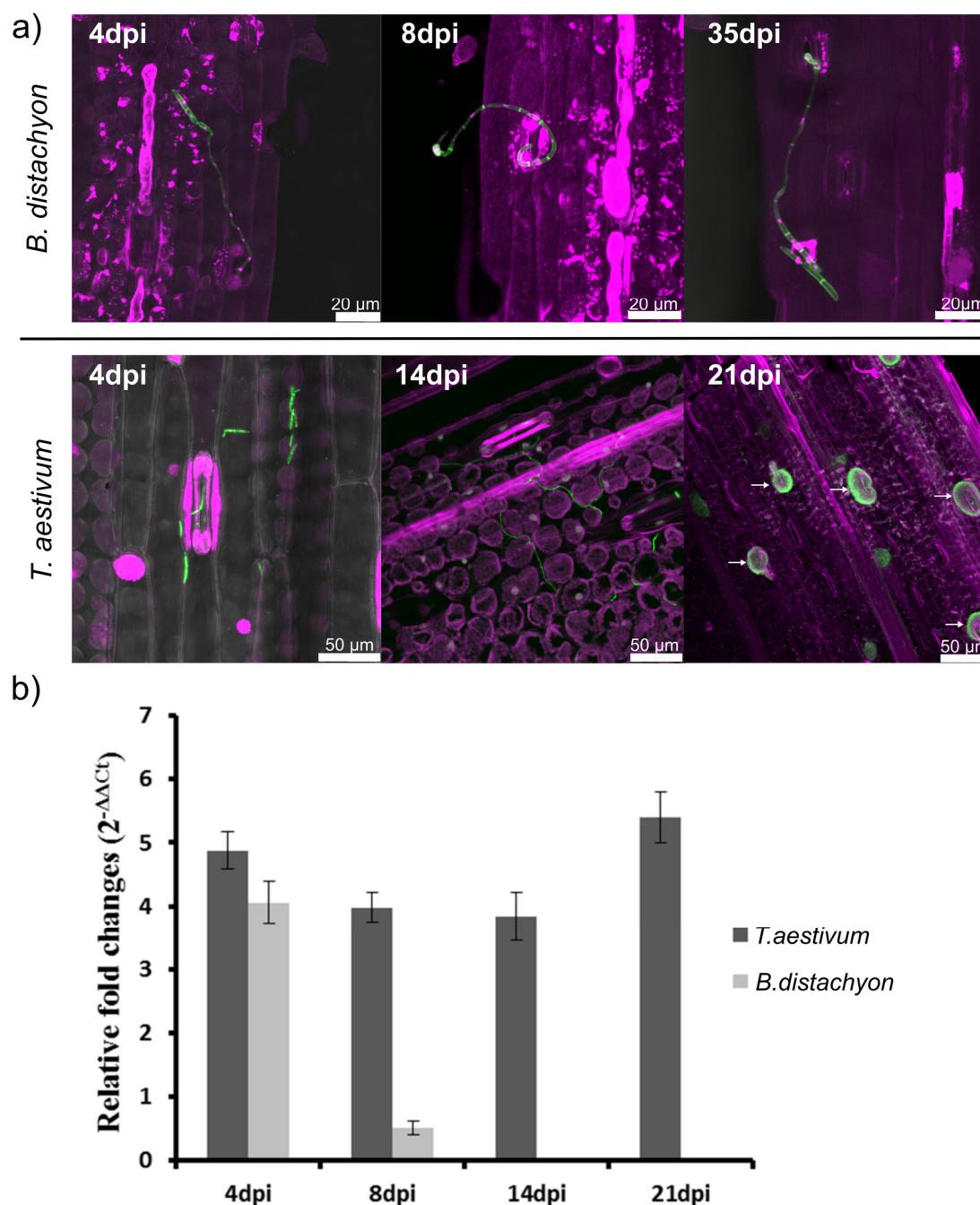
**Figure 2. *Z. tritici* infection hyphae are blocked in the substomatal cavities of *B. distachyon* which coincides with reduced expression of *Zt107320*.** a) Micrographs showing *Z. tritici* cells and emerging hyphae during penetration of *B. distachyon* stomata and infection of *T. aestivum*. On *T. aestivum*, *Z. tritici* germinated and penetrated the stomata at 4 dpi. Intercellular mesophyll colonization of *Z. tritici* occurred until 14 dpi resulting in the formation of pycnidia (indicated by arrows) at 21 dpi. In contrast, *Z. tritici* germinated on *B. distachyon* and penetrated stomata, but growth was halted below the stomata with no further leaf colonization (8 dpi - 35 dpi). Maximum projections of confocal image z-stacks. Nuclei and grass cells displayed in *purple* and fungal hyphae or septae respectively in *green*. b) Transcription of *Zt107320* in compatible (*T. aestivum)* and incompatible (*B. distachyon*) hosts. *In planta* expression of *Zt107320* is displayed relative to expression during axenic growth. Values are

9

177 normalized to the expression of the gene encoding the housekeeping protein GAPDH. Error bars

178 indicate the standard error of the mean (SEM) of three independent biological replicates per sample.

179

**Zt107320 is located with the nucleus during yeast-like growth**

181 The localization of Zt107320 within fungal cells was analysed using complementation strains that

182 expressed a Zt107320_eGFP fusion protein regulated by the native promotor. During yeast-like

183 growth on YMS media, the GFP-fusion protein appeared to be located in the nucleus or in its

184 immediate vicinity (see fig 3). This localization is similar to the reported nuclear localization of the

185 homolog AbPf1 (Cho *et al.* 2013) and supports the putative functional role of Zt107320 as a

186 transcription factor. The observed localisation of the Zt107320_eGFP fusion protein also verifies the

187 predicted nuclear localization of Zt107320 using the program WoLFPsort which implements an

188 algorithm for prediction of subcellular locations of proteins based on sequence composition and

189 content (Horton *et al.* 2007).

190



191
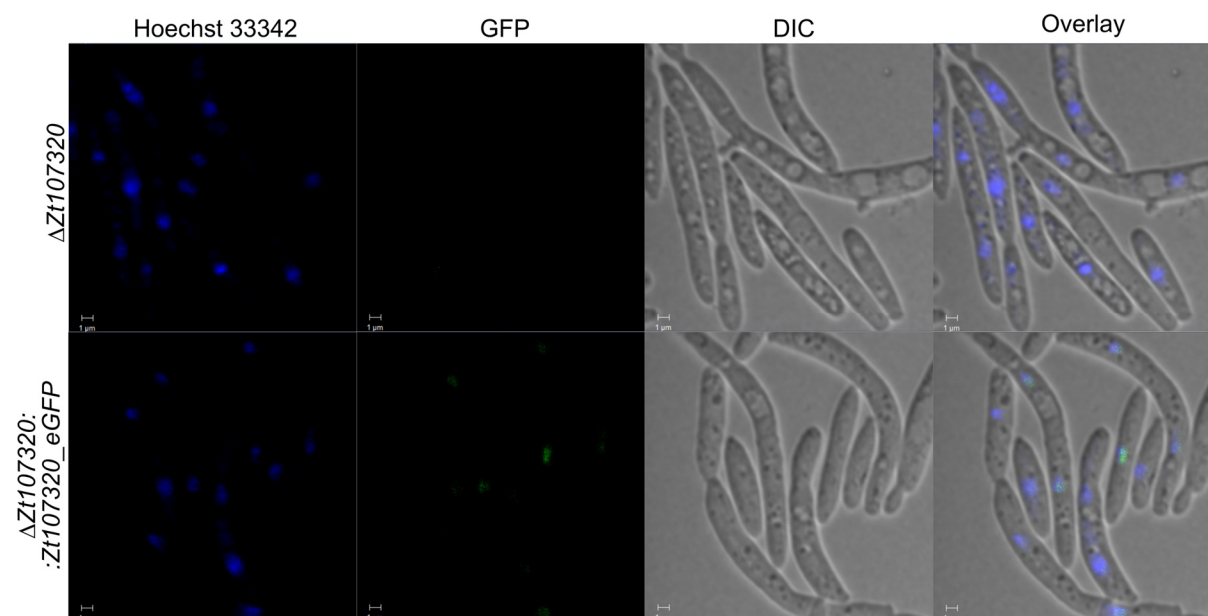
**Figure 3. Localization of the Zt107320_eGFP fusion protein detected by fluorescence microscopy**.
Nuclei were counterstained using the DNA-specific dye Hoechst33342. eGFP fluorescence co-localized with the Hoechst33342 signal indicating nuclear localization of the Zt107320_eGFP fusion protein. eGFP fluorescence is restricted to the nuclei (scale bars = 1 μm).

196

10

**Zt107320 regulates growth and affects cell wall properties**

Based on the coinciding halted growth and development and down-regulation of *Zt107320* in

incompatible infections, we next asked whether Zt107320 is involved in the regulation of growth of

*Z. tritici in vitro*. We determined the maximum growth rate r of *Z. tritici* in liquid cultures assuming a

logistic growth curve model. For two independently generated *Zt107320* deletion mutants, we

observed a significant reduction in the maximum growth rate compared to the wildtype. We thereby

confirm the relevance of *Zt107320* as a putative regulator for growth, as two complementation

strains showed no significant difference in the growth rate compared to the wildtype (fig 4a)

The effect of *Zt107320* deletion was not restricted to the growth rate but also included cell wall

properties. Compared to the wildtype, we observed reduced growth *in vitro* when challenging the

deletion mutants with high osmotic stresses (0.5 M and 1 M NaCl; 1 M, 1.5 M and 2 M Sorbitol) as

well as with cell wall stress agents (300 µg/mL and 500 µg/mL Congo red; 200 µg/mL Calcofluor).

Again, the wildtype phenotype was restored in both complementation strains (fig 4b and fig S1).

Interestingly, temperature stress (28°C) did not affect the wildtype and the deletion mutants

differently, as well as the exposure to $H_2O_2$ (1.5 mM and 2 mM). This indicates a specific effect of

*Zt107320* on the cell wall properties but not on the ability of the fungus to counteract reactive

oxygen species which are produced by the plant during activation of immune responses (Jones and

Dangl, 2006).



11
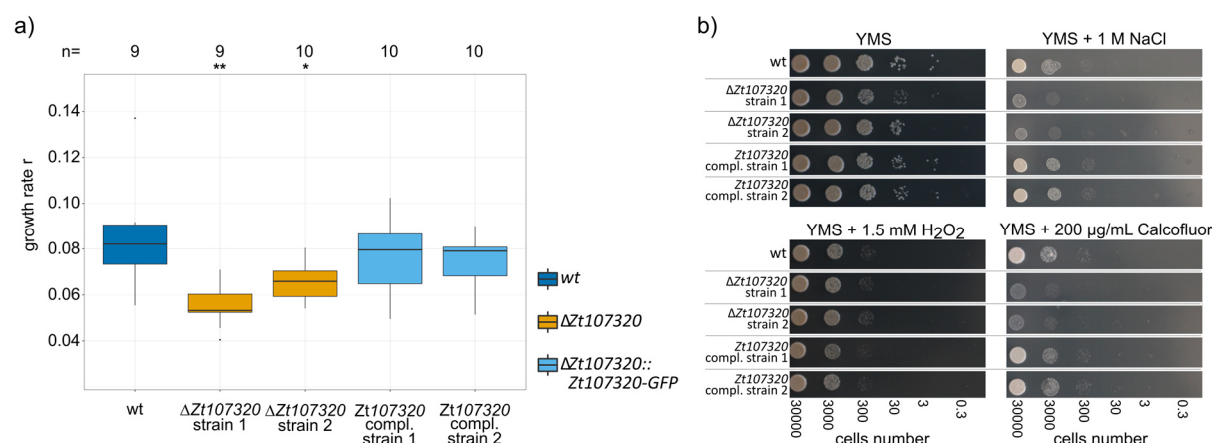
217 **Figure 4. Zt107320 regulates growth and affects cell wall properties of *Z. tritici*.** a) Maximum growth

218 rate in liquid culture. Statistical significance inferred through an ANOVA and subsequent post hoc

219 Tukey's HSD comparing the deletion and complementation strains to the wildtype, is indicated as *=

220 p <0.05; **= p<0.005; ***= p<0.0005. b) *In vitro* growth of the wildtype (wt), two deletion strains

221 (Δ*Zt107320*), two complementation strains (Δ*Zt107320*::*Zt107320*_eGFP) on YMS media including

222 the supplemented compounds to assess the role of osmotic stress (1 M NaCl), reactive oxygen

223 species (1.5 mM $H_2O_2$) and cell wall stressors (200 µg/mL Calcofluor).

224

225 The dimorphic switch from yeast-like to hyphal growth is considered to be central for pathogenicity

226 during the early stages of infection (Kema, G. H. J. *et al.* 1996; Yemelin *et al.* 2017). We therefore

227 next asked whether Zt107320 is involved in regulating this morphological switch of *Z. tritici.* To

228 promote hyphal growth we used minimal medium and supplied different carbon sources in order to

229 compare carbon utilisation and growth between the mutants and wildtype. Without carbon sources

230 as well as in the presence of cellulose as exclusive carbon source, *Z. tritici* showed solely hyphal

231 growth, indicating that carbon sources are required for yeast-like growth and that cellulose cannot

232 be utilized by the fungus. The wildtype *Z. tritici* strain showed markedly increased yeast-like growth

233 in the presence of the monosaccharides glucose, galactose, fructose and mannose as well as the

234 sugar alcohols sorbitol and mannitol. Increased growth was also observed in the presence of the

235 disaccharides sucrose and maltose (fig 5, fig S2). Interestingly, xylose as sole carbon source led to

236 predominant hyphal growth in the wild type strain, which contrasts to the mainly yeast-like growth

237 observed in the presence of all other tested carbohydrates. For xylose as sole carbon source, overall

238 growth is markedly increased compared to the minimal medium lacking a carbon source indicating

239 that xylose can be utilized by *Z. tritici* as a carbon source. The deletion of *Zt107320* affected fungal

240 growth morphology on all tested carbon sources. Compared to the wildtype and the

241 complementation strains, we observed increased hyphal growth for the Δ*Zt107320* strains on all

242 carbon sources after 14 days of incubation, except for cellulose (fig 5, fig S2). In particular,

243 supplementation of the monosaccharides fructose, glucose and xylose caused substantially

244 pronounced hyphal growth when *Zt107320* was deleted. The wildtype phenotype was restored in

245     both complementation strains confirming that *Zt107320* plays a role in the regulation of growth in *Z.*

246     *tritici*.
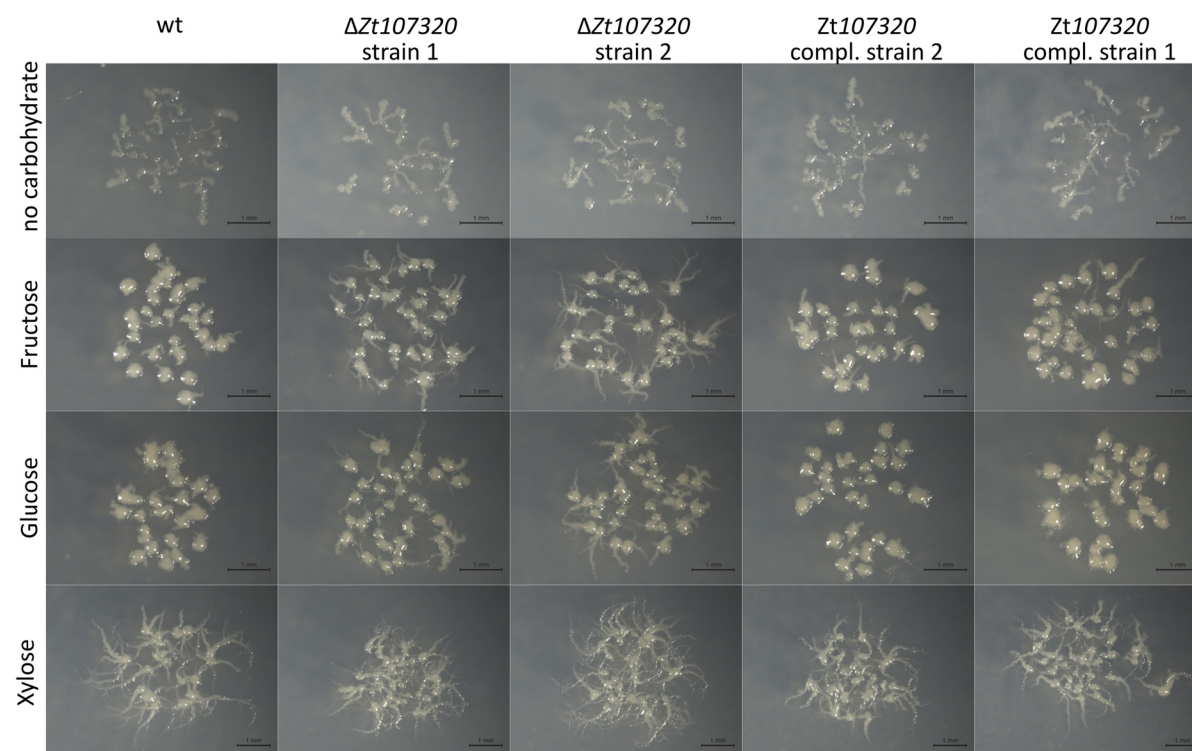


248     **Figure 5. Zt107320 regulates the dimorphic switch of *Z. tritici*.** Pictures showing morphologies of
249     colonies originating from single cells after 14 days of growth at 18°C on minimal media containing the
250     indicated carbohydrates as carbon sources. Fructose, glucose and xylose can be utilized by the fungus
251     and led to increased growth. The two strains in which *Zt107320* was deleted independently showed
252     an increase in hyphal growth compared to the wildtype, while in the two complementation strains
253     the wildtype colony morphology was restored.

254

255     **Zt107320 affects the ability of *Z. tritici* to produce pycnidia**

256     We next addressed whether the impact of *Zt107320* deletion on growth rate, the dimorphic switch

257     and cell wall properties also influence the ability of *Z. tritici* to infect its host, *T. aestivum*. We

258     inoculated a predefined area of the second leaf of the susceptible wheat cultivar Obelisk and

259     measured the number of pycnidia 21 days post infection. We observed a pronounced reduction in

260     the production of pycnidia for the *Zt107320* deletion strains. The density of pycnidia per $cm^2$ of

261     infected leaf area was reduced significantly for both independent deletions of *Zt107320* (ANOVA,

262     $p<1*10^{-7}$, p=0.002) (fig 6 a, b) compared to the wildtype. Complementing the *Zt107320* in-locus fully

13

263    restored the wildtype phenotype *in planta*. As the density of pycnidia is considered to be a

264    quantitative measure for virulence (Stewart *et al.* 2016), significantly decreased pycnidia production

265    indicates reduced virulence of mutants. Thus, we conclude that the putative transcription factor

266    Zt107320 by its effect on the growth rate, the dimorphic switch and the cell wall properties affects

267    the fitness of *Z. tritici* during infection of the compatible wheat host.



268
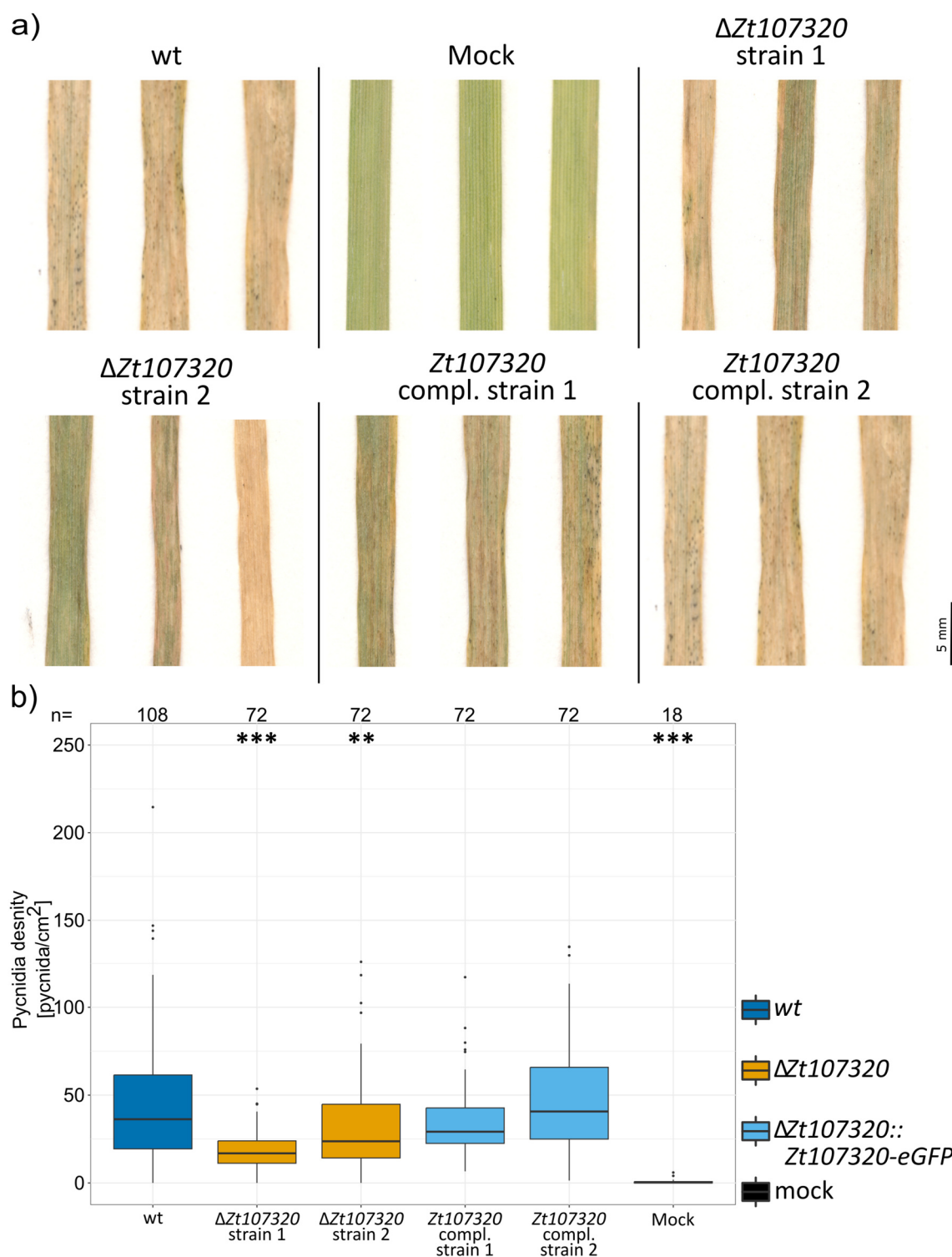
269 **Figure 6. *Zt107320* deletion affects the pycnidia production during a compatible infection of wheat.**

270 a) Pictures of representative leaves infected with the *Z. tritici* wildtype (wt), two deletion strains

271 (Δ*Zt107320*), two complementation strains (Δ*Zt107320*::*Zt107320-eGFP*) and mock-treated leaves. b)

272 Boxplot depicting the pycnidia density (pycnidia per cm$^2$ leaf) pooled for two independent

273 experiments. Number of leaves (N) for each strain is indicated on top. Statistical significance, inferred

274 through an ANOVA and subsequent post hoc Tukey's HSD comparing the deletion and

275 complementation strains to the wildtype, is indicated as *= p <0.05; **= p<0.005; ***= p<0.0005.

276

277

278 ## Discussion

279 Here, we show that the putative transcription factor Zt107320, belonging to the fungal Zn(II)$_2$Cys$_6$

280 family, is involved in the infection program of *Z. tritici* during a compatible interaction with the host

281 plant *T. aestivum*. Transcription of *Zt107320* is specifically induced during infection of wheat but not

282 during the infection of the non-host *B. distachyon*. This suggests a functional role of this gene in the

283 regulation of the infection program during a compatible host-pathogen interaction that allows the

284 fungus to overcome host defences and propagate in the mesophyll tissue.

285 To date, only a small number of genes have been shown to be involved in virulence of this important

286 wheat pathogen (Orton *et al.* 2011; Poppe *et al.* 2015). These genes encode the chitin binding LysM

287 effector Mg3LysM (Lee *et al.* 2014; Marshall *et al.* 2011) , two transcription factors ZtWor1 and ZtVf1

288 (Mirzadi Gohari *et al.* 2014; Mohammadi *et al.* 2017) and three rapidly evolving small proteins

289 (Hartmann *et al.* 2017; Poppe *et al.* 2015; Zhong *et al.* 2017). Indeed, multiple effector candidate

290 genes have been deleted but for most mutants no or small effects on pathogenicity were observed

291 (Gohari *et al.* 2015; Rudd *et al.* 2015). Therefore, a high level of functional redundancy seems to be

292 present in *Z. tritici*. The deletion of *Zt107320* results in a relatively small, nevertheless significant,

293 reduction of the pycnidia density which is in contrast to the fully or partially avirulent phenotype

294 demonstrated for the two previously deleted transcription factors ZtWor1 and ZtVf1, respectively

295 (Mirzadi Gohari *et al.* 2014; Mohammadi *et al.* 2017). Similar to our observation in the *Zt107320*

296 deletion mutant, deletion of *MoCOD1*, the rice blast homolog of *Zt107320*, led to a quantitative

297 reduction in lesion size and number (Chung *et al.* 2013). This partial, but incomplete, quantitative

15

298    reduction in virulence of *ΔZt107320* strains corresponds with the reduced, but still substantial

299    growth rate of these deletion mutants *in vitro*. Therefore, other mechanisms, independent of

300    Zt107320 are involved in the regulation of growth and development *in vitro* and *in planta*. Similarly, a

301    partial, but incomplete reduction of invasive growth *in planta* as observed in Δ*MoCOD1* (Chung *et al.*

302    2013). The impact of Zt107320 on fungal growth and pathogenicity is therefore similar to the effect

303    caused by other members of the Zn(II)$_2$Cys$_6$ transcription factor family: TPC1 regulates invasive,

304    polarized growth and virulence in the rice blast fungus *M. oryzae* (Galhano *et al.* 2017), and the

305    transcription factor FOW2 is known to control the ability of *F. oxysporum* to invade roots and

306    colonize plant tissue (Imazaki *et al.* 2007).

307    Zt107320 appears to be involved in the morphological switch from yeast-like to hyphal growth as

308    deletion of *Zt107320* led to an increase in hyphal growth. The switch to filamentous growth is

309    considered to be essential for plant infection (Kema, G. H. J. *et al.* 1996; Yemelin *et al.* 2017).

310    Therefore, the involvement of Zt107320 in regulating this dimorphism underscores its importance for

311    pathogenicity. Based on RT-qPCR data we observe that *Zt107320* is differentially expressed between

312    non-host and host infections and is further highly expressed during infections of compatible hosts.

313    Other RNAseq-based transcriptome studies found that *Zt107320* is upregulated during later stages of

314    wheat infection associated to necrotrophic host colonization, indicating a possible function for

315    pycnidia formation (Haueisen *et al.* 2019; Rudd *et al.* 2015). Together, these findings support a role

316    of Zt107320 in regulation of growth and pathogenicity of *Z. tritici*.

317    Interestingly, xylose the main product of hemicellulose degradation by fungal xylanases had a

318    pronounced effect on the growth pattern of Z. *tritici*. Xylose supplementation not only increased

319    overall growth compared to pure minimal medium but also led to an increase in the development of

320    filaments spanning larger distances. In *Z. tritici*, the switch to necrotrophic growth after an initial

321    phase of symptomless infection, overall disease severity and quantitative pycnidiospore production

322    are associated with the activity of endo-β-1,4-xylanase (Siah *et al.* 2010; Somai-Jemmali *et al.* 2017).

323    During the switch to necrotrophy *Z. tritici* rapidly develops large hyphal networks and uses plant-

16

324 derived nutrients (Haueisen *et al.* 2019; Rudd *et al.* 2015). The observed effect of xylose on the

325 growth morphology suggest that xylose – next to its role as a carbon source – may also direct growth

326 and promote the spatial expansion of the intrafoliar hyphal network during the fungal lifestyle switch

327 to necrotrophic growth. Indeed, genes encoding xylanases were shown to evolve under positive

328 selection (Brunner *et al.* 2013), indicating an important functional role of this class of enzymes for

329 adaptation to wheat infection. Although functional analyses of several xylanases in other plant

330 pathogenic fungi, resulted in no direct phenotypic effect (Brunner *et al.* 2013; Douaiher *et al.* 2007)

331 xylanases have been proposed as virulence factors (Douaiher *et al.* 2007). However, the results

332 presented here indicate a possible role of xylose as a host infection-associated signal molecule for *Z.*

333 *tritici* and should warrant further analysis.

334 In conclusion, we showed that Zt107320 affects the fitness of the wheat pathogen *Z. tritici*. *Zt107320*

335 is differentially expressed in host and non-host environments, being upregulated during the early

336 stages of infection on compatible hosts and down-regulated on non-hosts. This down-regulation

337 corresponds to a considerably reduced growth and halted infections of *Z. tritici* after stomatal

338 penetration of the non-host *B. distachyon*. In addition, we could confirm that Zt107320 has a nuclear

339 localisation, consistent with its putative function as a transcription factor and that it further regulates

340 the dimorphic switch between yeast-like and hyphal growth that is considered to be essential for

341 pathogenicity. We therefore hypothesize that the putative transcription factor Zt107320 is part of to

342 the regulatory network that controls host-associated growth and development, integrating signals

343 that differ between compatible and non-compatible infections. Future studies should address the

344 specific target genes of Zt107320 and their expression pattern during compatible and non-

345 compatible interactions. Furthermore, the transcriptional regulation of *Zt107320* suggests that

346 specific signals in the compatible host-pathogen interaction in wheat are responsible for the up-

347 regulation of this particular transcription factor-encoding gene. Identification of these host-derived

348 signals will provide fundamental insight into the molecular basis of host-pathogen interaction and

349 host specificity in *Z. tritici*.

17

350

## Experimental Procedures

352    **Fungal and plant strains**

353    The Dutch isolate IPO323 was kindly provided by Gert Kema (Wageningen, The Netherlands) and is

354    available from the Westerwijk Institute (Utrecht, The Netherlands) with the accession number CBS

355    115943. The strain used in our experiments lacked accessory chromosome 18, presumably lost

356    during culture maintenance *in vitro* (Kellner et al. 2014). Strains were maintained in either liquid

357    Yeast Malt Sucrose (YMS) broth (4 g/L Yeast extract. 4 g/L Malt extract, 4 g/L sucrose) at 18°C on an

358    orbital shaker or on solid YMS (+20 g/L agar) at 18°C. The *T. aestivum* cultivar Obelisk was obtained

359    from Wiersum Plantbreeding BV (Winschoten, The Netherlands). *B. distachyon* inbred line Bd21 was

360    kindly provided by Thierry Marcel (Bioger, INRA, France).

361

362    **Sequence analysis**

363    Phylogenetic analysis of Zt107320 was conducted using the software Geneious Prime 2019.0.4

364    (https://www.geneious.com). Homologues sequences to protein sequence of Zt107320 were

365    retrieved from the Fungal Transcription Factor Database (Park *et al.* 2008). Including Zt107320 and its

366    homologs from the sister species *Z. pseudotritici* and *Z. ardabiliae* a total of the 30 best matches

367    were retrieved. Alignments were constricted using MUSCLE (Edgar, 2004) and trees constructed

368    using Neighbour-Joining algorithm building a consensus tree using 1000 bootstrapping replicates.

369    Protein domains of the consensus sequence were identified using InterProScan (Quevillon *et al.*

370    2005). Prediction of the nuclear localisation of the Zt107320 was conducted using the WoLF PSORT

371    predictor (Horton *et al.* 2007).

372

373    **Analysis of *Z. tritici* during its compatible and non-compatible infections by confocal microscopy**

374  Morphology and development of *Z. tritici* inside and on the surface of leaves of B*. distachyon* inbred

375  line Bd21 were analysed by confocal laser-scanning microscopy (CLSM) as described previously

376  (Haueisen et al. 2019). Analyses of compatible *Z. tritici* infections on *Triticum aestivum* cultivar

377  Obelisk were conducted by combining microtomy and CLSM as previously described (Rath *et al.*

378  2014). Distinct areas of the second leaf of 12-day-old (Bd21) and 14-day-old (wheat) seedlings were

379  brush-inoculated with $1 \times 10^7$ cells/ml in 0.1% Tween 20. Plants were incubated at 22°C [day]/ 20°C

380  [night] and 100% humidity with a 16-h light period for 48 h. Subsequently, humidity was reduced to

381  70%. Microscopy was conducted using a Leica TCS SP5 and analysis of image z-stacks was done using

382  Leica Application Suite Advanced Fluorescence (Leica Microsystems, Germany) and AMIRA® (FEITM

383  Visualization Science Group, Germany).

384

385  **Analysis of Zt107320_eGFP expression using confocal microscopy.**

386  Cells were grown on solid YMS medium for 7 days before being scraped off the media surface and

387  introduced into 10 mM phosphate buffer (pH 7.2) containing 1 µg/µl Hoechst 33342 (Sigma-Aldrich

388  Chemie GmbH, Munich, Germany). Cells were incubated for 15-30 min in the dark and then

389  transferred to a microscope slide and analysed by confocal laser scanning microscopy.

390

391  **RNA isolation and quantitative RT-PCR**

392  We analysed gene expression patterns of *Zt107320* of *Z. tritici* employing a qRT-PCR experiment.

393  Total RNA was extracted from fungal axenic cultures (grown for 72 h in YMS medium at 18°C and 200

394  rpm) and from snap-frozen leaf tissue infected with *Z. tritici* (4, 8, 14 and 21 dpi) using the TRIZOL

395  reagent (Invitrogen, Karlsruhe, Germany), following the manufacturer's instructions. Three biological

396  replicates were included in the experimental set up. The cDNA samples were used in a qRT-PCR

397  experiment employing the iQ SYBR Green Supermix Kit (Bio-Rad, Munich, Germany). PCR was

398  conducted in a CFX96 RT-PCR Detection System (Bio-Rad, Munich, Germany) with the constitutively

19

399     expressed control gene Glyceraldehyde-3-phosphate dehydrogenase (GAPDH). All primers are listed

400     in table S1.

401     **Generation of Zt107320 deletion mutants and complementation by gene replacement**

402     Fungal transformations and the creation of knock-out and complementation mutants of *Zt107320*

403     were conducted as previously described (Poppe *et al.* 2015). In brief: Gene deletions were created by

404     amplifying an approximately 1 kb region of the 5' and 3' flanking regions of *Zt107320* using PCR. The

405     amplified flanking sequences were fused to a hygromycin resistance (hygR) cassette and an EcoRV

406     cut vector backbone (pES61) using Gibson assembly (Gibson *et al.* 2009). Electro-competent cells of

407     the *Agrobacterium tumefaciens* strains AGL1 were transformed using standard protocols. These

408     transformed *A. tumefaciens* cells were used for the transformation of *Z. tritici* as previously described

409     (Zwiers and De Waard, Maarten A. 2001). The same strategy was applied for the creation of the

410     complementation strains by a C-terminal fusion of the *Zt107320* gene with an eGFP tag and a

411     geneticin resistance cassette as a selection marker (fig. S3). After transformation and homologous

412     recombination in the Δ*Zt107320* strain 1, the hygromycin resistance cassette was replaced by

413     *Zt107320-eGFP* and the geneticin resistance cassette (NeoR) (fig. S3). Homologous recombination

414     and integration was confirmed using PCR and Southern blot analysis by standard protocols. In short,

415     genomic DNA was isolated using Phenol-Chloroform isolation (Sambrook and Russell, 2001).

416     Restriction digestion was performed using PvuII, followed by gel-electrophoresis, blotting and

417     detection using Dig-labelled probes binding to the upstream and downstream flank of *Zt107320* (fig.

418     S2). In total four Δ*Zt107320* strains, and two Δ*Zt107320*::*Zt107320*-eGFP strains were created.

419

420     **Isolation of fungal DNA and Southern blot analysis**

421     DNA was isolated using phenol/chloroform applying a protocol previously described (Sambrook and

422     Russell, 2001). Transformants were first screened using a PCR based approach detecting the

423     resistance cassette and the endogenous locus. Candidate transformants were further confirmed by

424     Southern blot analysis using a standard protocol (Southern, 1975). Probes were generated using the

20

425      PCR DIG labelling Mix (Roche, Mannheim, Germany) according to the manufacturer's instructions

426      (Table S1).

427

428      *In vitro* **phenotyping**

429      The *Z. tritici* strains were grown on YMS solid medium for 5-7 days at 18°C before the cells were

430      scraped from the plate surface. For the determination of the growth rate, the cells were resuspended

431      and counted. The cell density was adjusted to 50000 cells/mL and 175µl of the cell suspension was

432      added to a well of a 96 well plate. Plates were inoculated at 18°C at 200 rpm with the OD600 being

433      measured twice daily on a Multiskan Go plate reader (Thermo Scientific, Dreieich, Germany) (Table

434      S2). Estimation of the growth rate was done by employing the logistic growth equation as

435      implemented in the growthcurver package (version 0.2.1) in R (version R3.4.1) (R Core Team, 2015).

436      For the determination of the *in vitro* phenotypes, the cell number was adjusted to $10^7$ cells/mL in

437      ddH$_2$O and serially diluted to $10^3$ cells/mL. 3 µL of each cell dilution was transferred onto YMS agar

438      including the tested compounds and incubated for seven days at 18°C or 28°C. To test high osmotic

439      stresses 0.5 M NaCl, 1 M NaCl, 1M Sorbitol, 1.5 M Sorbitol, 2 M Sorbitol (obtained from Carl Roth

440      GmbH, Karlsruhe, Germany) were added to the YMS solid medium. To test cell wall stresses 300

441      µg/mL and 500 µg/mL Congo red and 200 µg/mL Calcofluor (obtained from Sigma-Aldrich Chemie

442      GmbH, Munich, Germany) were added to the YMS solid medium. Finally, to determine the effect of

443      reactive oxygen species on the mutant growth morphology 2 mM H$_2$O$_2$ (obtained from Carl Roth

444      GmbH, Karlsruhe, Germany) was added to the YMS solid medium.

445      To test whether the Zt107320 affects the hyphal growth of *Z. tritici* and the ability of the fungus to

446      use different carbon sources we used minimum media (MM) as described in (Barratt *et al.* 1965).

447      Glucose, fructose, xylose, mannose, galactose, sorbitol, mannitol, sucrose and cellulose were added

448      at a final concentration of 10 g/L and 20g/L agar were included. Strains were grown on YMS solid

449      medium for 7 days and scraped into ddH2O, the cell number adjusted to $10^7$, $10^6$, $10^5$, $10^4$, $10^3$

21

450     cells/mL and 3 µl of each cell concentration added to the surface of the minimum medium plates.

451     Plates were incubated 18°C in the dark and the growth monitored after 7 days and 14 days.

452

453     ***In planta* phenotyping**

454     For the *in planta* phenotypic assays, we germinated seeds of the wheat cultivar Obelisk on wet sterile

455     whatman paper for four days before potting using the soil Fruhstorfer Topferde (Hermann Meyer

456     GmbH, Rellingen, Germany). Wheat seedlings were further grown for seven days before inoculation.

457     *Z. tritici* strains were grown in YMS solid medium for five days at 18°C before the cells were scraped

458     from the plate surface. The cell number was adjusted to $10^8$ cells/mL in $H_2O$ + 0.1% Tween 20, and

459     the cell suspension was brushed onto approximately five cm on the abaxial and adaxial sides of the

460     second leaf of each seedling. Inoculated plants were placed in sealed bags containing water for 48 h

461     to facilitate infection through stomata. Plants were grown under constant conditions with a day night

462     cycle of 16h light (~200µmol/m$^2$*s) and 8h darkness in growth chambers at 20°C. Plants were grown

463     for 21 days post inoculation at 90% relative humidity (RH). At 21 dpi the infected leaves were cut and

464     taped to sheets of paper and pressed for five days at 4°C before being scanned at a resolution of

465     2400 dpi using a flatbed scanner (HP photosmart C4580, HP, Böblingen, Germany). Scanned images

466     were analysed using an automated image analysis in Image J (Schneider *et al.* 2012) adapted from

467     (Stewart *et al.* 2016). The read-out pycnidia/cm$^2$ leaf surface was used for all subsequent analyses.

468     See Table S3 for summary of *in planta* results.

469

470     **Statistical analysis**

471     Statistical analyses were conducted in R (version R3.4.1) (R Core Team, 2015) using the suite R Studio

472     (version 1.0.143) (RStudio Team, 2015). Data inspection showed a non-normal distribution for all

473     data sets, including the measured pycnidia density (pycnidia/cm$^2$). Therefore, we performed an

474     omnibus analysis of variance using rank-transformation of the data (Conover and Iman, 1981)

22

475    employing the model: pycnidia density ~ strain * experiment and r ~ strain, respectively. Post hoc

476    tests were performed using Tukey's HSD (Tukey, 1949).

477

## Acknowledgements

483


## References

485 **Barratt, R.W. Johnson, G.B. and Ogata, W.N.** (1965) Wild-type and mutant stocks of Aspergillus
486    nidulans. *Genetics,* **52**, 233.
487 **Brading, P.A. Verstappen, Els C P, Kema, Gert H J and Brown, James K M** (2002) A Gene-for-Gene
488    Relationship Between Wheat and Mycosphaerella graminicola, the Septoria Tritici Blotch
489    Pathogen. *Phytopathology,* **92**, 439–445.
490 **Brunner, P.C. Torriani, S. F. F. Croll, D. Stukenbrock, E.H. and McDonald, B.A.** (2013) Coevolution
491    and Life Cycle Specialization of Plant Cell Wall Degrading Enzymes in a Hemibiotrophic Pathogen.
492    *Molecular Biology and Evolution,* **30**, 1337–1347.
493 **Chen, Y. Le, X. Sun, Y. Li, M. Zhang, H. Tan, X. Zhang, D. Liu, Y. and Zhang, Z.** (2017) MoYcp4 is
494    required for growth, conidiogenesis and pathogenicity in Magnaporthe oryzae. *Mol. Plant Pathol.*
495    **18**, 1001–1011.
496 **Cho, Y. Ohm, R.A. Grigoriev, I.V. and Srivastava, A.** (2013) Fungal-specific transcription factor AbPf2
497    activates pathogenicity in Alternaria brassicicola. *The Plant journal : for cell and molecular biology,*
498    **75**, 498–514.
499 **Chung, H. Choi, J. Park, S.-Y. Jeon, J. and Lee, Y.-H.** (2013) Two conidiation-related Zn(II)2Cys6
500    transcription factor genes in the rice blast fungus. *Fungal Genet. Biol.* **61**, 133–141.
501 **Conover, W.J. and Iman, R.L.** (1981) Rank transformations as a bridge between parametric and
502    nonparametric statistics. *The American Statistician,* **35**, 124–129.
503 **Douaiher, M.-N. Nowak, E. Durand, R. Halama, P. and Reignault, P.** (2007) Correlative analysis of
504    Mycosphaerella graminicola pathogenicity and cell wall-degrading enzymes produced in vitro: the
505    importance of xylanase and polygalacturonase. *Plant Pathology,* **56**.
506 **Edgar, R.C.** (2004) MUSCLE. Multiple sequence alignment with high accuracy and high throughput.
507    *Nucleic Acids Res,* **32**, 1792–1797.
508 **Fones, H. and Gurr, S.** (2015) The impact of Septoria tritici Blotch disease on wheat: An EU
509    perspective. *Fungal genetics and biology : FG & B,* **79**, 3–7.
510 **Fox, E.M. Gardiner, D.M. Keller, N.P. and Howlett, B.J.** (2008) A Zn(II)2Cys6 DNA binding protein
511    regulates the sirodesmin PL biosynthetic gene cluster in Leptosphaeria maculans. *Fungal Genet.*
512    *Biol.* **45**, 671–682.

23

513    **Galhano, R. Illana, A. Ryder, L.S. Rodríguez-Romero, J. Demuez, M. Badaruddin, M. Martinez-**
514    **Rocha, A.L. Soanes, D.M. Studholme, D.J. Talbot, N.J. and Sesma, A.** (2017) Tpc1 is an important
515    Zn(II)2Cys6 transcriptional regulator required for polarized growth and virulence in the rice blast
516    fungus. *PLoS Pathog,* **13**, e1006516.

517    **Gibson, D.G. Young, L. Chuang, R.-Y. Venter, J.C. Hutchison, C.A. and Smith, H.O.** (2009) Enzymatic
518    assembly of DNA molecules up to several hundred kilobases. *Nature methods,* **6**, 343–345.

519    **Gohari, A.M. Ware, S.B. Wittenberg, Alexander H J, Mehrabi, R. M'Barek, S.B. Verstappen, Els C P,**
520    **van der Lee, Theo A J, Robert, O. Schouten, H.J. de Wit, Pierre P J G M and Kema, G.H.** (2015)
521    Effector discovery in the fungal wheat pathogen Zymoseptoria tritici. *Molecular Plant Pathology,*
522    **16**, 931–945.

523    **Grandaubert, J. Dutheil, J.Y. and Stukenbrock, E.H.** (2017) The genomic determinants of adaptive
524    evolution in a fungal pathogen.

525    **Habig, M. Kema, G. and Holtgrewe Stukenbrock, E.** (2018) Meiotic drive of female-inherited
526    supernumerary chromosomes in a pathogenic fungus.

527    **Hartmann, F.E. Sanchez-Vallet, A. McDonald, B.A. and Croll, D.** (2017) A fungal wheat pathogen
528    evolved host specialization by extensive chromosomal rearrangements. *The ISME journal,* **11**,
529    1189–1204.

530    **Haueisen, J. Möller, M. Eschenbrenner, C.J. Grandaubert, J. Seybold, H. Adamiak, H. and**
531    **Stukenbrock, E.H.** (2019) Highly flexible infection programs in a specialized wheat pathogen.
532    *Ecology and evolution,* **9**, 275–294.

533    **Horton, P. Park, K.-J. Obayashi, T. Fujita, N. Harada, H. Adams-Collier, C.J. and Nakai, K.** (2007)
534    WoLF PSORT. Protein localization predictor. *Nucleic Acids Res,* **35**, W585-7.

535    **Imazaki, I. Kurahashi, M. Iida, Y. and Tsuge, T.** (2007) Fow2, a Zn(II)2Cys6-type transcription
536    regulator, controls plant infection of the vascular wilt fungus Fusarium oxysporum. *Molecular*
537    *microbiology,* **63**, 737–753.

538    **Jing, H.-C. Lovell, D. Gutteridge, R. Jenk, D. Kornyukhin, D. Mitrofanova, O.P. Kema, Gert H. J. and**
539    **Hammond-Kosack, K.E.** (2008) Phenotypic and genetic analysis of the Triticum monococcum-
540    Mycosphaerella graminicola interaction. *New Phytol.* **179**, 1121–1132.

541    **Jones, J.D.G. and Dangl, J.L.** (2006) The plant immune system. *Nature,* **444**, 323–329.

542    **Kellner, R. Bhattacharyya, A. Poppe, S. Hsu, T.Y. Brem, R.B. and Stukenbrock, E.H.** (2014) Expression
543    Profiling of the Wheat Pathogen Zymoseptoria tritici Reveals Genomic Patterns of Transcription
544    and Host-Specific Regulatory Programs. *Genome Biol Evol,* **6**, 1353–1365.

545    **Kema, G.H. Verstappen, E.C. Todorova, M. and Waalwijk, C.** (1996) Successful crosses and molecular
546    tetrad and progeny analyses demonstrate heterothallism in Mycosphaerella graminicola. *Curr*
547    *Genet,* **30**, 251–258.

548    **Kema, G. H. J. Yu, D.Z. Rijkenberg, F. H. J. Shaw, M.W. and Baayen, R.P.** (1996) Histology of the
549    pathogenesis of Mycosphaerella graminicola in wheat. *Phytopathology 86: 777-786*.

550    **Lee, W.-S. Rudd, J.J. Hammond-Kosack, K.E. and Kanyuka, K.** (2014) Mycosphaerella graminicola
551    LysM effector-mediated stealth pathogenesis subverts recognition through both CERK1 and CEBiP
552    homologues in wheat. *Molecular plant-microbe interactions : MPMI,* **27**, 236–243.

553    **Lu, J. Cao, H. Zhang, L. Huang, P. and Lin, F.** (2014) Systematic analysis of Zn2Cys6 transcription
554    factors required for development and pathogenicity by high-throughput gene knockout in the rice
555    blast fungus. *PLoS Pathog,* **10**, e1004432.

556    **MacPherson, S. Larochelle, M. and Turcotte, B.** (2006) A fungal family of transcriptional regulators:
557    the zinc cluster proteins. *Microbiology and molecular biology reviews : MMBR,* **70**, 583–604.

558    **Marshall, R. Kombrink, A. Motteram, J. Loza-Reyes, E. Lucas, J. Hammond-Kosack, K.E. Thomma,**
559    **Bart P H J and Rudd, J.J.** (2011) Analysis of two in planta expressed LysM effector homologs from

560    the fungus Mycosphaerella graminicola reveals novel functional properties and varying
561    contributions to virulence on wheat. *Plant Physiol.* **156**, 756–769.

562    **Mirzadi Gohari, A. Mehrabi, R. Robert, O. Ince, I.A. Boeren, S. Schuster, M. Steinberg, G. de Wit,**
563    **Pierre J. G. M. and Kema, Gert H. J.** (2014) Molecular characterization and functional analyses of
564    ZtWor1, a transcriptional regulator of the fungal wheat pathogen Zymoseptoria tritici. *Molecular*
565    *Plant Pathology,* **15**, 394–405.

566    **Mohammadi, N. Mehrabi, R. Gohari, A.M. Mohammadi Goltapeh, E. Safaie, N. and Kema, G.H.J.**
567    (2017) The ZtVf1 transcription factor regulates development and virulence in the foliar wheat
568    pathogen Zymoseptoria tritici. *Fungal Genetics and Biology,* **109**, 26–35.

569    **Möller, M. Habig, M. Freitag, M. and Stukenbrock, E.H.** (2018) Extraordinary Genome Instability and
570    Widespread Chromosome Rearrangements During Vegetative Growth. *Genetics*.

571    **Morais, D. Gélisse, S. Laval, V. Sache, I. and Suffert, F.** (2016) Inferring the origin of primary
572    inoculum of Zymoseptoria tritici from differential adaptation of resident and immigrant
573    populations to wheat cultivars. *Eur J Plant Pathol,* **145**, 393–404.

574    **O'Driscoll, A. Doohan, F. and Mullins, E.** (2015) Exploring the utility of Brachypodium distachyon as a
575    model pathosystem for the wheat pathogen Zymoseptoria tritici. *BMC Res Notes,* **8**, 132.

576    **Okmen, B. Collemare, J. Griffiths, S. van der Burgt, Ate, Cox, R. and Wit, P.J.G.M.** de (2014)
577    Functional analysis of the conserved transcriptional regulator CfWor1 in Cladosporium fulvum
578    reveals diverse roles in the virulence of plant pathogenic fungi. *Molecular microbiology,* **92**, 10–
579    27.

580    **Orton, E.S. Deller, S. and Brown, James K M** (2011) Mycosphaerella graminicola: from genomics to
581    disease control. *Mol. Plant Pathol.* **12**, 413–424.

582    **Pan, T. and Coleman, J.E.** (1990) GAL4 transcription factor is not a" zinc finger" but forms a Zn (II)
583    2Cys6 binuclear cluster. *Proc. Natl. Acad. Sci. U.S.A.* **87**, 2077–2081.

584    **Park, J. Park, J. Jang, S. Kim, S. Kong, S. Choi, J. Ahn, K. Kim, J. Lee, S. Kim, S. Park, B. Jung, K. Kim, S.**
585    **Kang, S. and Lee, Y.-H.** (2008) FTFD. An informatics pipeline supporting phylogenomic analysis of
586    fungal transcription factors. *Bioinformatics (Oxford, England),* **24**, 1024–1025.

587    **Ponomarenko A. S.B. Goodwin, G.H.J. Kema** (2011) Septoria tritici blotch (STB) of wheat.
588    *10.1094/PHI*.

589    **Poppe, S. Dorsheimer, L. Happel, P. and Stukenbrock, E.H.** (2015) Rapidly Evolving Genes Are Key
590    Players in Host Specialization and Virulence of the Fungal Wheat Pathogen Zymoseptoria tritici
591    (Mycosphaerella graminicola). *PLoS pathogens,* **11**, e1005055.

592    **Quevillon, E. Silventoinen, V. Pillai, S. Harte, N. Mulder, N. Apweiler, R. and Lopez, R.** (2005)
593    InterProScan. Protein domains identifier. *Nucleic Acids Res,* **33**, W116-20.

594    **R Core Team** (2015) R: A Language and Environment for Statistical Computing. Vienna, Austria.
595    https://www.R-project.org.

596    **Rath, M. Grolig, F. Haueisen, J. and Imhof, S.** (2014) Combining microtomy and confocal laser
597    scanning microscopy for structural analyses of plant-fungus associations. *Mycorrhiza,* **24**, 293–
598    300.

599    **RStudio Team** (2015) RStudio: Integrated Development Environment for R. Boston, MA.
600    http://www.rstudio.com/.

601    **Rudd, J.J. Kanyuka, K. Hassani-Pak, K. Derbyshire, M. Andongabo, A. Devonshire, J. Lysenko, A.**
602    **Saqi, M. Desai, N.M. Powers, S.J. Hooper, J. Ambroso, L. Bharti, A. Farmer, A. Hammond-Kosack,**
603    **K.E. Dietrich, R.A. and Courbot, M.** (2015) Transcriptome and metabolite profiling of the infection
604    cycle of Zymoseptoria tritici on wheat reveals a biphasic interaction with plant immunity involving
605    differential pathogen chromosomal contributions and a variation on the hemibiotrophic lifestyle
606    definition. *PLANT PHYSIOLOGY,* **167**, 1158–1185.

607 **Rybak, K. See, P.T. Phan, H.T.T. Syme, R.A. Moffat, C.S. Oliver, R.P. and Tan, K.-C.** (2017) A
608     functionally conserved Zn2 Cys6 binuclear cluster transcription factor class regulates necrotrophic
609     effector gene expression and host-specific virulence of two major Pleosporales fungal pathogens
610     of wheat. *Mol. Plant Pathol.* **18**, 420–434.

611 **Sambrook, J. and Russell, D.W.** (2001) Molecular Cloning. A laboratory manual. Gold Spring Harbor,
612     New York: Gold Spring Harbor Laboratory Pr.

613 **Schneider, C.A. Rasband, W.S. and Eliceiri, K.W.** (2012) NIH Image to ImageJ. 25 years of image
614     analysis. *Nat Meth,* **9**, 671–675.

615 **Siah, A. Deweer, C. Duyme, F. Sanssené, J. Durand, R. Halama, P. and Reignault, P.** (2010)
616     Correlation of in planta endo-beta-1,4-xylanase activity with the necrotrophic phase of the
617     hemibiotrophic fungus Mycosphaerella graminicola. *Plant Pathology,* **59**, 661–670.

618 **Somai-Jemmali, L. Randoux, B. Siah, A. Magnin-Robert, M. Halama, P. Reignault, P. and Hamada,**
619     **W.** (2017) Similar infection process and induced defense patterns during compatible interactions
620     between Zymoseptoria tritici and both bread and durum wheat species. *Eur J Plant Pathol,* **147**,
621     787–801.

622 **Son, H. Seo, Y.-S. Min, K. Park, A.R. Lee, J. Jin, J.-M. Lin, Y. Cao, P. Hong, S.-Y. Kim, E.-K. Lee, S.-H.**
623     **Cho, A. Lee, S. Kim, M.-G. Kim, Y. Kim, J.-E. Kim, J.-C. Choi, G.J. Yun, S.-H. Lim, J.Y. Kim, M. Lee,**
624     **Y.-H. Choi, Y.-D. and Lee, Y.-W.** (2011) A phenome-based functional analysis of transcription
625     factors in the cereal head blight fungus, Fusarium graminearum. *PLoS Pathog.* **7**, e1002310.

626 **Southern, E.M.** (1975) Detection of specific sequences among DNA fragments separated by gel
627     electrophoresis. *Journal of Molecular Biology,* **98**, 503–517.

628 **Stewart, E.L. Hagerty, C.H. Mikaberidze, A. Mundt, C.C. Zhong, Z. and McDonald, B.A.** (2016) An
629     Improved Method for Measuring Quantitative Resistance to the Wheat Pathogen Zymoseptoria
630     tritici Using High-Throughput Automated Image Analysis. *Phytopathology,* **106**, 782–788.

631 **Tukey, J.W.** (1949) Comparing Individual Means in the Analysis of Variance. *Biometrics,* **5**, 99.

632 **Xiong, D. Wang, Y. Tang, C. Fang, Y. Zou, J. and Tian, C.** (2015) VdCrz1 is involved in microsclerotia
633     formation and required for full virulence in Verticillium dahliae. *Fungal Genet. Biol.* **82**, 201–212.

634 **Yemelin, A. Brauchler, A. Jacob, S. Laufer, J. Heck, L. Foster, A.J. Antelo, L. Andresen, K. and Thines,**
635     **E.** (2017) Identification of factors involved in dimorphism and pathogenicity of Zymoseptoria
636     tritici. *PLoS ONE,* **12**, e0183065.

637 **Zhang, W.-Q. Gui, Y.-J. Short, D.P.G. Li, T.-G. Zhang, D.-D. Zhou, L. Liu, C. Bao, Y.-M. Subbarao, K.V.**
638     **Chen, J.-Y. and Dai, X.-F.** (2018) Verticillium dahliae transcription factor VdFTF1 regulates the
639     expression of multiple secreted virulence factors and is required for full virulence in cotton. *Mol.*
640     *Plant Pathol.* **19**, 841–857.

641 **Zhong, Z. Marcel, T.C. Hartmann, F.E. Ma, X. Plissonneau, C. Zala, M. Ducasse, A. Confais, J.**
642     **Compain, J. Lapalu, N. Amselem, J. McDonald, B.A. Croll, D. and Palma-Guerrero, J.** (2017) A
643     small secreted protein in Zymoseptoria tritici is responsible for avirulence on wheat cultivars
644     carrying the Stb6 resistance gene. *The New phytologist,* **214(2)**, 619–631.

645 **Zhuang, Z. Lohmar, J.M. Satterlee, T. Cary, J.W. and Calvo, A.M.** (2016) The Master Transcription
646     Factor mtfA Governs Aflatoxin Production, Morphological Development and Pathogenicity in the
647     Fungus Aspergillus flavus. *Toxins,* **8**.

648 **Zwiers, L.-H. and De Waard, Maarten A.** (2001) Efficient Agrobacterium tumefaciens-mediated gene
649     disruption in the phytopathogen Mycosphaerella graminicola. *Current Genetics,* **39**, 388–393.

650

651

652 **Supporting Information legends**

653

654 **Figure S1. In vitro phenotype of *Zt107320* mutants.** I*n vitro* growth of the wildtype (wt), two

655 independent deletion strains (Δ*Zt107320*), two independent complementation strains

656 (Δ*Zt107320*::*Zt107320*_eGFP) on YMS media including the indicated compounds to assess the effect

657 of osmotic stress (NaCl, Sorbitol) , reactive oxygen species ($H_2O_2$),  cell wall stressors (Calcofluor,

658 Congo Red) and increased temperature (28°C) on growth and morphology of *Z. tritici.*

659

660 **Figure S2. Growth morphologies of Z. tritici wildtype and Δ*Zt107320* and Δ*Zt107320::Zt107320-***

661 ***eGFP* strains on minimum medium in the presence of different carbon sources.** Growth depicted

662 after a) 7 days and b) 14 days**.** After 7 days, and more pronounced after 14 days of incubation, a

663 higher amount of hyphal growth is observed for the Δ*Zt107320* mutants on the carbon sources

664 Fructose, Galactose, Glucose, Maltose, Sorbitol, Sucrose and Xylose.

665

666 **Figure S3. Generation of *Zt107320* mutants in *Z. tritici***. a) Schematic illustration of the gene

667 replacement strategy of *Zt107320*.  Generation of the Δ*Zt107320* strains by homologous

668 recombination between the upstream (UF) and downstream flanking regions (DF) of *Zt107320* in its

669 genomic locus and a plasmid carrying the hygromycin resistance cassette (hygR) located between the

670 UF and DF. Homologous recombination results in the integration of the hygromycin-resistance gene

671 cassette (*hygR*) in the locus of *Zt107320*. Δ*Zt107320::Zt107300*-eGFP were generated by homologous

672 recombination between UF and DF of the Δ*Zt107320* strains and a transformed plasmid containing a

673 c-terminal fusion of *Zt107320* and *eGFP* and a Geneticin resistance cassette (*NeoR*) located between

674 the UF and DF Yellow bars indicate the position of the probes used in the Southern blot analyses. b)

675 Confirmation of *Zt107320* mutants by Southern blot analyses.

676

677 **Table S1: List of all primers used within this study**

678 **Table S2: Summary of *in vitro* growth data**

679 **Table S3: Summary of *in planta* phenotype**